Edinburgh Research Explorer

Simulation of a solid sorption ice-maker based on the novel composite sorbent "lithium chloride in silica gel pores"

Simulation of a solid sorption ice-maker based on the novel composite sorbent "lithium chloride in silica gel pores"

G. Maggio[a*], L. G. Gordeeva[b], A. Freni[a], Yu. I. Aristov[b],

G. Santori[c], F. Polonara[c], G. Restuccia[a]

[a]*CNR - Istituto di Tecnologie Avanzate per l'Energia "Nicola Giordano",*
Via Salita S. Lucia sopra Contesse 5, 98126 Santa Lucia, Messina, Italy.

[b]*Boreskov Institute of Catalysis, Siberian Division, Russian Academy of Sciences,*
Pr. Akademika Lavrentieva 5, Novosibirsk 630090, Russia.

[c] *Università Politecnica delle Marche, Facoltà di Ingegneria, Dipartimento di Energetica,*
Via Brecce Bianche, Monte Dago, 60131 Ancona, Italy.

* Corresponding author. Tel.: +39-90-624243; fax: +39-90-624247.
E-mail address: gaetano.maggio@itae.cnr.it

Abstract

In this paper, a novel composite sorbent "lithium chloride in silica gel pores" is proposed for application in solar-powered adsorptive ice makers. A mathematical model was used in order to calculate the performance of an ice-maker using this material as adsorbent and methanol as adsorbate. The results of the model showed that a maximum solar Coefficient Of Performance (COPs) of 0.33 and a maximum Daily Ice Production (DIP) of 20 kg m^{-2} can be obtained for an ice-maker equipped with a solar collector area of 1.5 m^2 and 36 kg of adsorbent material. Such performance are noticeably higher than those obtained using commercial activated carbon, that is the adsorbent mostly proposed till now.

Nomenclature

A_i (i=1-5, 9)	Heat transfer surface, m^2
c	Specific heat, $J\,kg^{-1}\,K^{-1}$
$COPs$	Solar Coefficient Of Performance
DIP	Daily Ice Production, kg
I_β	Available solar radiation @ β=30°, $W\,m^{-2}$
K_i (i=1-3)	Flag: 0 or 1 (see Eqs. (2) and (9))
L_a	Adsorbate latent heat of condensation/evaporation $J\,kg^{-1}$
L_w	Water latent heat of solidification, $J\,kg^{-1}$
m	Mass, kg
m_a	Initial adsorbate mass inside evaporator, kg
m_w	Liquid water mass, kg
n	Solar collector area, m^2
p	Pressure, Pa
T	Temperature, K
t	Time, s
t_{cycle}	Cycle time, s
U_i (i=1-9)	Global heat transfer coefficient, $W\,m^{-2}\,K^{-1}$
w	Uptake, $kg\,kg^{-1}$

Greek letters

$(\tau\alpha)_{eff}$	Transmittance/absorptivity coefficient
ΔH	Adsorption/desorption enthalpy, $J\,kg^{-1}$

ΔT	Variation of temperature, K
Δw	Variation of uptake, $kg\,kg^{-1}$

Subscripts

1	Solar collector/environment
2	Solar collector/adsorbent
3	Condenser/environment
4	Evaporator/liquid water
5	Environment/liquid water
6	Evaporator/phase-changing water
7	Evaporator/solid water
8	Environment/solid water
9	Evaporator/environment
a	Adsorbate
ads	Adsorption
amb	Ambient
c	Condenser
des	Desorption
eq	Equivalent
ev	Evaporator
ice	Iced water
lw	Liquid water
m	Solar collector
s	Solid adsorbent material (dry)
w	Water
β	Tilt angle

Superscripts

C	Closed ventilation windows
O	Open ventilation windows

1. Introduction

A solar-powered adsorptive ice-maker consists of a small size adsorbent reactor connected to a solar collector, for regeneration of the sorbent material during the day, and connected to an evaporator, for ice production during the night [1-2]. Different prototypes were realized, showing the potentiality of this technology [2-5].

In particular, Sumathy and Li [2-3] designed and tested in Hong Kong a solar adsorption ice-maker with a single flat-plate collector (0.92 m^2 exposed area), based on activated carbon/methanol pair. Their experiments showed that this system can produce 4.3-5.4 kg m^{-2} day^{-1} of ice, with a solar COP of 0.10-0.12. These values are in good agreement with those reported by M. Li [4] for a similar flat-plate ice-maker tested in Shanghai: 4.7-6.7 kg m^{-2} day^{-1} of ice and a COP of 0.12-0.15, for a solar collector of

0.75 m^2. Anyanwu and Ezekwe [5] designed, constructed and tested in Nsukka,

Nigeria, a flat-type solar adsorption refrigerator using activated carbon/methanol, with

effective exposed area of 1.2 m^2. They obtained a maximum solar COP of 0.02, but this

low value was attributed to the "non-selective collector plate surface coating used".

Recently, Khattab [6] proposed and tested an innovative modular ice-maker with the

adsorbent (granular carbon bonded with blackened steel) placed in a glass container,

positioned between reflector panels. This system, using methanol as adsorbate, provided

a COP of 0.16 and a daily ice production of 9.4 kg m^{-2} day^{-1}. S.G. Wang and R.Z. Wang

[7] reported a COP of 0.18 for a sophisticated two-bed adsorption prototype ice-making

machine operating with heat and mass recovery and based on activated carbon/methanol

pair.

Several authors estimated the performance of adsorption ice-makers by mathematical

modelling [8-13]. The solar COP and the DIP calculated by simulations ranged between

0.10-0.12 and 4-10 kg m^{-2} day^{-1}, respectively. Such results are in good agreement with

those obtained by testing experimental prototypes.

It must be pointed out that most of the ice-makers presented in literature use

conventional activated carbon as adsorbent. The adsorption capacity of activated

carbons is rather low and usually does not exceed 30-40 wt.%.

The utilization of novel adsorbent materials with improved methanol sorption ability

can be an efficient way to increase the performance of the system. Recently, the

Boreskov Institute of Catalysis, Novosibirsk, Russia in collaboration with the CNR-

ITAE, Messina, Italy, developed a new class of methanol composite sorbents [14, 15].

This new class of sorbents is directly derived by the SWSs (Selective Water Sorbents;

i.e. a composite materials consisting of "inorganic salts confined to porous matrices"),

that have already been proposed for water vapour sorption [16]. The synthesised

composite sorbents demonstrated a strong affinity to methanol. Indeed, the maximal

amount of methanol sorbed w_{max}=75-80 wt.% exhibited by some composites is much higher that the methanol sorption capacity of conventional activated carbons [17]. This great enhancement of adsorptivity is due to the high contribution of methanol absorption by the salt embedded in the silica gel porous matrix (see [15] for details). Among the different composites synthesised, the sorbent "Lithium Chloride in mesoporous silica gel" (2-50 nm pore diameter) appeared to be the best candidate for sorption cooling driven by a low temperature energy source [18].

The aim of this paper is to evaluate the performance of a solar-powered adsorptive ice-maker using the novel composite "Lithium Chloride in mesoporous silica gel" by applying the simulation tool presented in Ref. [19].

The model makes it possible to calculate the performance of the unit in terms of solar Coefficient Of Performance (COPs), Daily Ice Production (DIP) and equivalent Daily Ice Production (DIP$_{eq}$). The obtained performance are compared with those corresponding to the commercial adsorbent activated carbon AC35. In the first part of the paper, the main features of the composite sorbent and of the simulated adsorptive unit are presented. Then, performance of the adsorptive ice-maker are calculated.

2. Main features of the composite sorbent "Lithium Chloride in mesoporous silica gel"

The composite sorbent "Lithium Chloride in mesoporous silica gel" (salt content 29.5 wt.%) was synthesised by impregnation of silica gel Grace Davison 8926.02 (average pore diameter d_{av} = 15 nm, specific surface S_{sp} = 326 m^2 g^{-1}, pore volume V_p = 1.5 cm^3 g^{-1}) with an aqueous solution of Lithium Chloride. More details on the synthesis procedure were presented by Gordeeva et al. [15]. Figure 1 shows the basic thermodynamic cycles for an adsorption air conditioner (T_{ev}=10 °C, T_c=T_{ads}=35 °C, T_{des}=80 °C) and an ice-maker (T_{ev}=−2 °C, T_c=T_{ads}=30 °C, T_{des}=80 °C) using the

4

composite "Lithium Chloride in mesoporous silica" and the commercial activated carbon AC35.

The cycles are plotted over an isosteric diagram that was obtained from the experimental equilibrium data presented in Refs. [15, 20] (only the significant isosters are plotted). It is evident that this novel composite sorbent presents an outstanding variation of methanol uptake per cycle (Δw= 46 wt.% and 18 wt.% for air conditioning and ice-making, respectively), which is much larger than those of the conventional carbon AC35 (Δw= 11 wt.% and 9 wt.% for air conditioning and ice-making, respectively). This is a convenient feature, because the performance of adsorptive machines increase when the amount of cycled working fluid increases [17].

The stability of adsorbent is of primary importance for evaluation of practical potential. Study on the phase composition, porous structure, and sorption properties of both the fresh and tested composites showed that no significant change, in composite structure and sorption ability, occurs during the cycling. Further details can be found in [21]. Furthermore, the stability to the cyclic treatment has been verified for this typology of materials [22]. A stability of the porous structure of the solid adsorbent, identical to the material studied in this paper, has been evidenced, even after thousands of cycles.

3. Description of the ice-maker

The scheme of the solar-powered adsorptive ice-maker is presented in Fig. 2. It consists of the following components: a solar collector, in which the adsorbent material is embedded; a condenser for the methanol condensation and the heat rejection to the ambient during the day; a "cold chamber", containing the evaporator for the methanol evaporation and the liquid water to be frozen during the night.

We selected a flat planar panel because the proposed working pair is able to efficiently work with this type of solar collector. Moreover, the niche application for this system (ice production in remote areas) asks for employment of cheap components.

During the day, the solar energy received by the collector produces the desorption of methanol from the sorbent bed. Methanol vapour flows to the condenser, condenses, and then is collected inside the receiver. During this phase the valves V_1 and V_2 are closed (see Fig. 2). In the late afternoon the valve V_1 is opened, and the liquid methanol flows from the receiver to the evaporator. Then, V_1 is closed and V_2 is opened for the whole night, allowing adsorption of methanol by the sorbent layer. The evaporation of methanol inside the cold chamber cools down the liquid water, which is converted into ice.

The adsorbent/adsorbate working pair follows the typical adsorptive cycle, consisting of four phases [23]: I) isosteric heating until the pressure reaches p_c; II) desorption at high temperature and pressure of condensation; III) isosteric cooling until the pressure decreases down to p_{ev}; IV) adsorption at low temperature and pressure of evaporation. During this last phase, three sub-steps may occur: IVa) cooling of the liquid water inside the cold box, IVb) freezing of the liquid water, IVc) under-cooling of the ice.

4. Modelling

The model is of dynamic type and is based on energy and mass balances for the adsorbent reactor and the connected components. The main governing equations are:

Solar collector:

$$n(\tau\,\alpha)_{eff}\,I_\beta = m_m c_m \frac{dT_m}{dt} + U_2 A_2\left(T_m - T_s\right) + U_1^{C/O} A_1\left(T_m - T_{amb}\right) \qquad \textbf{(1),}$$

where $U_1^{C/O}$ is equal to U_1^{C} or U_1^{O} for heating and cooling phases, respectively.

Adsorbent bed:

$$U_2 A_2 \left(T_m - T_s\right) = \left(m_s c_s + w m_s c_a\right) \frac{dT_s}{dt} - K_1 \, m_s \Delta H(w) \frac{dw}{dt} \tag{2},$$

with $K_1=0$ for isosteric phases and $K_1=1$ for isobaric phases.

Condenser:

$$L_a \left(T_c\right) m_s \frac{dw}{dt} = -m_c \, c_c \frac{dT_c}{dt} - U_3 A_3 \left(T_c - T_{amb}\right) \tag{3},$$

Evaporator:

$$L_a \left(T_{ev}\right) m_s \frac{dw}{dt} = -U_\alpha A_4 \left(T_{ev} - T_w\right) - \left[m_{ev} \, c_{ev} + \left(m_a - \Delta w \, m_s\right) c_a\right] \frac{dT_{ev}}{dt} - U_9 A_9 \left(T_{ev} - T_{amb}\right) \tag{4},$$

Water/ice heat and mass balances:

$$m_w c_w \frac{dT_w}{dt} = U_\alpha A_4 \left(T_{ev} - T_w\right) + U_\beta A_5 \left(T_w - T_{amb}\right) \tag{5},$$

$$L_w \frac{dm_{ice}}{dt} = L_a \left(T_{ev}\right) m_s \frac{dw}{dt} \tag{6},$$

where $U_\alpha = U_4$, $U_\beta = U_5$ and $c_w = c_{lw}$ for Step IVa;

$U_\alpha = U_6$ for Step IVb;

$U_\alpha = U_7$, $U_\beta = U_8$ and $c_w = c_{ice}$ for Step IVc.

Further supplementary equations are reported in a previous paper [19].

The accompanying initial conditions and starting values are:

$$\begin{cases} T_m(0) = T_s(0) = T_{amb}(0) \\ p_s(0) = p_{ev} \\ w(0) = w_2 \end{cases} \tag{7},$$

$$\begin{cases} T_c\left(t_1\right) = T_{amb}\left(t_1\right) \\ T_{ev}\left(t_3\right) = T_w\left(t_3\right) = T_{ev,0} \\ m_{ice}\left(t_{4a}\right) = 0 \end{cases} \tag{8},$$

where p_{ev} is calculated from the initial evaporator temperature, w_2 is calculated from the initial temperature and pressure of the adsorber, t_1 is the time of the end of Phase I (and start of Phase II), t_3 is the time of the end of Phase III (and start of Step IVa), t_{4a} is the time of the end of Step IVa (and start of Step IVb) and $T_{ev,0}$ is the initial evaporator temperature.

Depending on the phase of the thermodynamic cycle, only a certain number of the previous equations (1)-(6) is applied and the relative coefficients/parameters assume a different form (see [19] for details).

The end phase conditions are the following:

Phase I: $p_s = p_c$;   Phase II: $I_\beta < 100 \ W \ m^{-2}$ or $w \leq 2\%$;   Phase III: $p_s = p_{ev}$;

Step IVa: $T_w = 0$ or $t = 24$ h;   Step IVb: $m_{ice} = m_w$ or $t = 24$ h;   Step IVc: $t = 24$ h.

Furthermore, for each day, the corresponding solar Coefficient Of Performance (COPs) is calculated as:

$$COPs = \frac{Useful \ effect}{Available \ solar \ energy} = \frac{m_w \ c_{lw} \ \Delta T_w\big|_{step \ IVa} + K_2 \ m_{ice} \ L_w + K_3 \ m_w \ c_{ice} \ \Delta T_w\big|_{step \ IVc}}{n \int_0^{t_{cycle}} I_\beta(t) \, dt}$$

$$(9),$$

where $K_2 = 0$ and/or $K_3 = 0$ when Step IVb and/or IVc does not occur.

This definition of solar COP is identical to that reported in other literature works (see, in particular, Refs. [5] and [24]).

The Daily Ice Production (DIP) and its equivalent value (DIP$_{eq}$), which accounts for the equivalent mass of ice corresponding to the possible under-cooling of the ice, are given by

$$DIP = K_2 \ m_{ice} \qquad\qquad\qquad (10),$$

and

$$DIP_{eq} = DIP \left(1 + \frac{m_w \, c_{ice} \, \Delta T_w \big|_{step \, IVc}}{m_{ice} \, L_w} \right) \qquad \textbf{(11).}$$

The model equations were numerically solved by using a commercial software (Mathematica® 4.0 by Wolfram Research) for ordinary differential equation (ODE) systems, based on a function which automatically switches between stiff (Gear) and non-stiff (Adams) integration methods [25].

5. Results and comments

5.1. Results of a base-case

A base-case was assumed considering an adsorption ice-maker with a solar collector area n=1.5 m^2, mass of adsorbent material m_s= 36 kg, mass of liquid water inside the cold chamber m_w=20 kg. The simulations were carried out for a long period, considering as adsorbent material the activated carbon AC35 and the composite sorbent "lithium chloride in silica gel pores". Results are here presented for a few days of an intermediate season. Figure 3 shows the values of the dynamic data (useful solar radiation I_β and ambient temperature T_{amb}) for the six-day period considered for simulations (May 1-6, 2005). The data were recorded by a meteo-station installed at the CNR-ITAE in Messina, Italy (38° 12' N). From this figure, it results that the daily ambient temperature ranges from 13.7 °C to 23.6 °C; while the daily average useful solar radiation is about 500 W m^{-2}, with a maximum daily radiation ranging from 970 W m^{-2} to 1055 W m^{-2}. The third day, i.e. May 3, 2005 showed the lowest ambient temperature, but the day that exhibits the most instable climatic conditions is May 6, 2005.

 In Figs. 4 and 5 the calculated temperatures of the adsorbent material and of the condenser are presented for the activated carbon AC35 and the "LiCl silica gel" sorbent, respectively. Figure 4 shows that the maximum daily temperature reached by the activated carbon is 78°C (on May the 2nd), while the lowest daily temperature is 57°C,

due to the unfavourable conditions on May the 6th. The condenser temperature was always slightly higher than the ambient temperature.

The temperature evolution calculated for the composite sorbent "LiCl in silica gel" is rather different (see Fig. 5). Indeed, the sorbent maximum daily temperature is lower, ranging from 47°C to 57°C. This effect can be explained considering that a big part of the incoming radiant energy is required for rejection of the high amount of methanol sorbed by the composite. Besides, the higher content of methanol inside the adsorbent bed leads to higher thermal capacity, which contributes to increase the sensible heat of the system.

Correspondingly, the methanol uptake variation per day, Δw, ranged from 9 to 20 wt.%, for the case of AC35, and from 20 to 35 wt.%, for the case of the composite sorbent "LiCl in silica gel". This confirms the better sorption properties for the proposed sorbent with respect to the commercial carbon.

Figures 6, 7 show the calculated values of the temperature of methanol inside the evaporator and the mass of water converted into ice, inside the cold chamber. It can be observed that the system based on activated carbon (Fig. 6) is not able to produce 20 kg (i.e. 13.3 kg m^{-2}) of ice every day, and the corresponding temperature is higher than -5 °C. On the contrary, the system based on "LiCl in silica gel" (Fig. 7) demonstrated a capability of Daily Ice Production of 20 kg and a lower evaporation temperature (-10 °C is the minimum). Only for the first day the DIP is lower than 20 kg (18.6 kg, i.e. 12.4 kg m^{-2}); this is due to the low adsorbent temperature (see Fig. 5) and the corresponding high uptake, that are affected by the weather conditions of the previous (not represented) days. The temperature of the water in the cold chamber is almost coincident with that of evaporation, due to the good thermal contact between liquid methanol and water.

Inspection of Fig. 7 shows that, in the case of the system based on "LiCl in silica gel", the evaporator is significantly under-cooled after the production of 20 kg of ice. Subsequently, it can be argued that this system could be able to produce a further amount of ice (i.e., more than 20 kg day^{-1}=13.3 kg m^{-2} day^{-1}). Therefore the potentiality of this material, for ice-making applications, deserves a deeper investigation that is described in the next paragraph.

5.2. Calculation of performance

The performance were calculated considering an ice-maker with the same design of the above described base-case and different amounts of liquid water to be frozen. The Daily Ice Production (DIP), its equivalent value (DIP$_{eq}$) and the daily Coefficient Of Performance (COPs), were calculated according to Eqs. (9)-(11). Afterwards, the average values of these parameters ($\overline{DIP}$, $\overline{DIP_{eq}}$ and $\overline{COPs}$), corresponding to the whole period considered for simulations, were determined. Figure 8 reports the $\overline{DIP_{eq}}$ (in kg m^{-2}) calculated for the two adsorbents. The values of ice production calculated for the system based on activated carbon/methanol pair (7.5-11 kg m^{-2} day^{-1}) are in good agreement with the values reported in literature for this configuration [7, 12-13]. It is evident that the adsorption ice-maker based on AC35 provides a maximum of 11 kg m^{-2} day^{-1} of ice, due to the limited adsorption capacity of the carbon. Furthermore, this value decreases when the amount of liquid water in the cold chamber increases, due to the higher liquid water sensible heat.

Thus the optimum amount of liquid water to put in the cold box is about 19 kg for the AC35-CH$_3$OH pair. This value is much higher (about 37 kg of water) for the LiCl-CH$_3$OH pair, with a corresponding maximum of 20 kg m^{-2} day^{-1} of ice production. This is evidently due to the higher adsorption capacity of the composite sorbent.

Figure 9 reports the $\overline{COPs}$ calculated for the two adsorbents. It results that the average

solar COP corresponding to the system using activated carbon is equal to 0.17,

independently on the liquid water mass. This result, which is coherent with the values

reported by other authors [6, 7, 10, 12], confirms that the use of activated carbon cannot

ensure the design of a highly performing adsorption ice-maker. Differently, the COPs of

the system based on Lithium Chloride increases when liquid water mass increases, and

reaches a noticeable value of 0.33, which is almost twice the maximum value obtained

for AC35.

These results clearly demonstrate that the outstanding methanol sorption properties of

the composite sorbent "LiCl in silica gel" make possible the realization of an adsorption

ice-maker which performs much better than the units previously proposed in literature

and that is potentially attractive for the niche-market of the solar cooling in remote

areas.

The COP and DIP values previously reported in literature for activated carbon/methanol

systems represent a preliminary validation of the proposed model, which should be

definitely accomplished when the measured performance parameters of a prototype,

based also on the other adsorbent/adsorbate pair, will be available. This will be done in

a following paper.

6. Conclusions

This study evidences that the utilization of innovative adsorbent materials with high

sorption ability can improve the performance of adsorptive cooling systems. In

particular, it was shown that the novel composite sorbent "Lithium Chloride in silica gel

pores" makes it possible to design highly efficient solar-powered adsorptive ice-makers.

Indeed, mathematical modelling demonstrated that a maximum solar Coefficient Of

Performance (COPs) of 0.33 and a maximum Daily Ice Production (DIP) of 20 kg m^{-2}

can be obtained for an ice-maker using a solar collector area of 1.5 m^2 and 36 kg of "Lithium Chloride in silica gel pores" sorbent. Such performance are more than 80% higher than those obtained using common activated carbon.

References

[1]   A. Dieng, R.Z. Wang, Literature review on solar adsorption technologies for ice-making and air-conditioning purposes and recent developments in solar technology, Renewable & Sustainable Energy Reviews 5 (4) (2001) 313-342.

[2]   Z.F. Li, K. Sumathy, A solar powered ice-maker with the solid adsorption pair of activated carbon and methanol, International Journal of Energy Research 23 (6) (1999) 517-527.

[3]   K. Sumathy, L. Zhongfu, Experiments with solar-powered adsorption ice-maker, Renewable Energy 16 (1-4) (1998) 704-707.

[4]   M. Li, R.Z. Wang, Y. Xu, J. Wu, A. Dieng, Experimental study on dynamic performance analysis of a flat-plate solar solid-adsorption refrigeration for ice maker, Renewable Energy 27 (2) (2002) 211-221.

[5]   E.E. Anyanwu, C.I. Ezekwe, Design, construction and test run of a solid adsorption solar refrigerator using activated carbon/methanol, as adsorbent/adsorbate pair, Energy Conversion & Management 44 (18) (2003) 2879-2892.

[6]   N.M. Khattab, Simulation and optimization of a novel solar-powered adsorption refrigeration module, Solar Energy 80 (2006) 823-833.

[7]   S.G. Wang, R.Z. Wang, Recent developments of refrigeration technology in fishing vessels, Renewable Energy 30 (2005) 589-600.

[8]   M. Li, R.Z. Wang, Heat and mass transfer in a flat plate solar solid adsorption refrigeration ice maker, Renewable Energy 28 (4) (2003) 613-622.

[9] Y.J. Dai, K. Sumathy, Heat and mass transfer in the adsorbent of a solar adsorption cooling system with glass tube insulation, Energy 28 (14) (2003) 1511-1527.

[10] E.F. Passos, J.F. Escobedo, F. Meunier, Simulation of an intermittent adsorptive solar cooling system, Solar Energy 42 (2) (1989) 103-111.

[11] E.J. Hu, R.H.B. Exell, Simulation and sensitivity analysis of an intermittent solar powered charcoal/methanol refrigerator, Renewable Energy 4 (1) (1994) 133-149.

[12] A. Boubakri, J. Guilleminot, F. Meunier, Adsorptive solar powered ice-maker: experiments and model, Solar Energy 69 (3) (2000) 249-263.

[13] A.P.F. Leite, M. Daguenet, Performance of a new solid adsorption ice maker with solar energy, Energy Conversion & Management 41 (15) (2000) 1625-1647.

[14] Yu.I. Aristov, L.G. Gordeeva, Yu.D. Pankratiev, L.M. Plyasova, I.V. Bikova, A. Freni, G. Restuccia, Sorption Equilibrium of Methanol on new composite sorbents "CaCl$_2$/Silica Gel", Adsorption 13 (2) (2007) 121-127.

[15] L.G. Gordeeva, A. Freni, T.A. Krieger, G. Restuccia, Yu.I. Aristov, Composites "lithium halides in silica gel pores": methanol sorption equilibrium, Microporous and Mesoporous Materials 112 (1-3) (2008) 254-261.

[16] Yu.I. Aristov, G. Restuccia, G. Cacciola, V.N. Parmon, A family of new working materials for solid sorption air conditioning systems, Applied Thermal Engineering 22 (2) (2002) 191-204.

[17] L.G. Gordeeva, A. Freni, G. Restuccia, Yu.I. Aristov, A new family of methanol sorbents for adsorptive air conditioning driven by low temperature heat in: Proceedings of the International Conference on Heat Powered Cycles, Newcastle upon Tyne, 11-14 September 2006, pp. 21-22.

[18] L.G. Gordeeva, A. Freni, G. Restuccia, Yu.I Aristov, Influence of characteristics of methanol sorbents "salt in mesoporous silica" on the performance of adsorptive

air conditioning cycle, Industrial & Engineering Chemistry Research 46 (9) (2007) 2747-2752.

[19] S. Vasta, G. Maggio, G. Santori, A. Freni, F. Polonara, G. Restuccia, An adsorptive solar ice-maker dynamic simulation for north Mediterranean climate, Energy Conversion & Management, accepted for publication 2008.

[20] G. Restuccia, Yu.I. Aristov, G. Maggio, G. Cacciola, M.M. Tokarev, Performance of sorption systems using new selective water sorbents in: Proceedings of the International Sorption Heat Pump Conference, Munich, 24-26 March 1999, pp. 219-223.

[21] A. Freni, L.G. Gordeeva, S. Vasta, Yu. I. Aristov, G. Restuccia, Composite sorbent of methanol "lithium chloride in mesoporous silica gel" for adsorptive cooling machines: performance evaluation, International Symposium on Innovative Materials for Processes in Energy Systems (IMPRES), 28-31 October, 2007, Kyoto, Japan; paper ID: A035.

[22] G. Restuccia, S. Vasta, A. Freni, F. Russo, Yu. I. Aristov, An advanced solid sorption chiller using SWS-1L: performance analysis and hydrothermal cycling stability of the sorbent bed, in: Proceedings of the International Sorption Heat Pump Conference, June 22-24, 2005, Denver, CO, USA; paper # ISHPC-078-2005. http://www.enme.umd.edu/ceee/ishpc/content/ISHPC2005Proceedings.pdf

[23] G. Cacciola, G. Restuccia, Reversible adsorption heat pump: a thermodynamic model, International Journal of Refrigeration 18 (2) (1995) 100-106.

[24] H.L. Luo, Y.J. Dai, R.Z. Wang, R. Tang, M. Li, Year round test of a solar adsorption ice maker in Kunming, China, Energy Conversion and Management 46 (13-14) (2005) 2032-2041.

[25] K. Radhakrishnan, A.C. Hindmarsh, Description and use of LSODE, the Livermore Solver for Ordinary Differential Equations in: Lawrence Livermore National Laboratory technical report UCRL-ID-113855, March 1994.

FIGURE CAPTIONS

Figure 1: Comparison between the composite sorbent "Lithium Chloride in mesoporous silica gel" and the activated carbon AC35, in terms of air conditioning and ice-making cycles.

Figure 2: Scheme of the solar-powered adsorptive ice-maker.

Figure 3: Ambient temperature and solar radiation recorded in May 1-6, 2005.

Figure 4: Condenser and adsorbent temperature, calculated for activated carbon and 20 kg of liquid water.

Figure 5: Condenser and adsorbent temperature, calculated for LiCl in silica gel and 20 kg of liquid water.

Figure 6: Evaporator temperature and mass of ice calculated for activated carbon and 20 kg of liquid water.

Figure 7: Evaporator temperature and mass of ice calculated for LiCl in silica gel and 20 kg of liquid water.

Figure 8: Equivalent Daily Ice Production vs. liquid water mass, calculated for the two adsorbents.

Figure 9: Average Solar Coefficient Of Performance vs. liquid water mass, calculated for the two adsorbents.
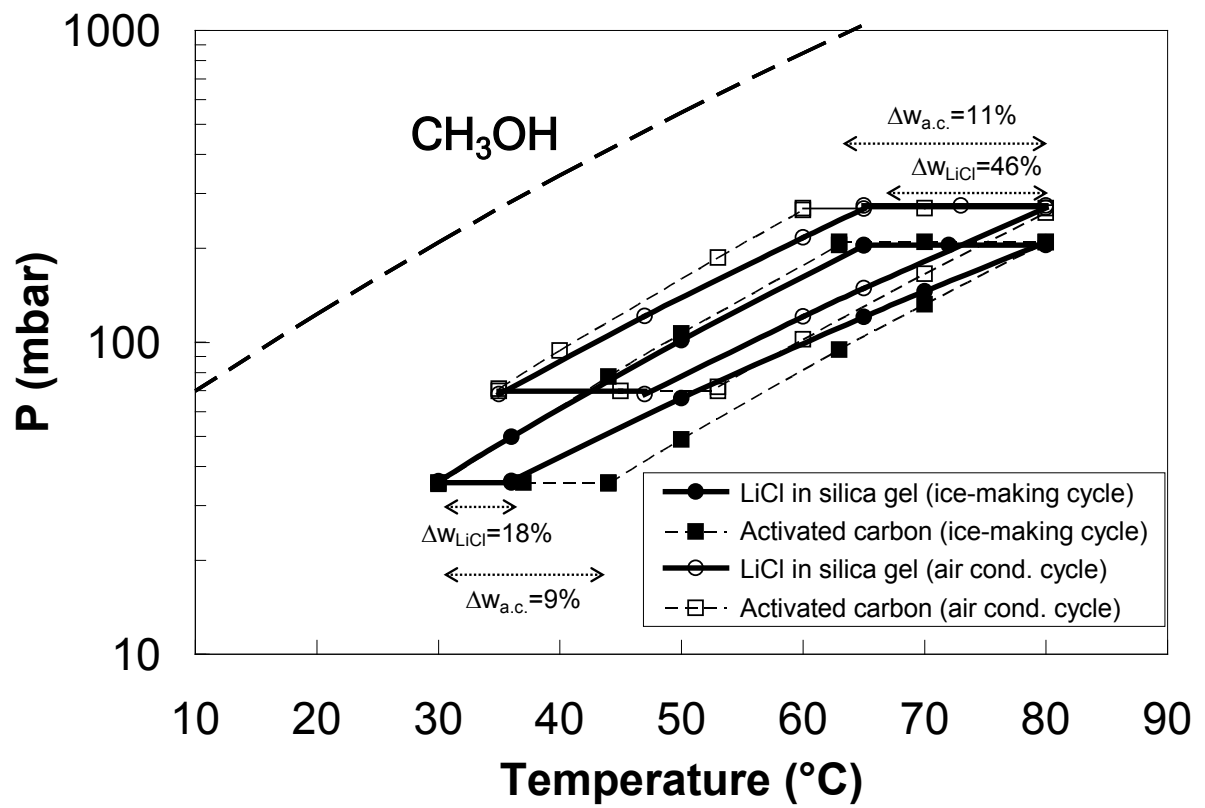
Figure 1
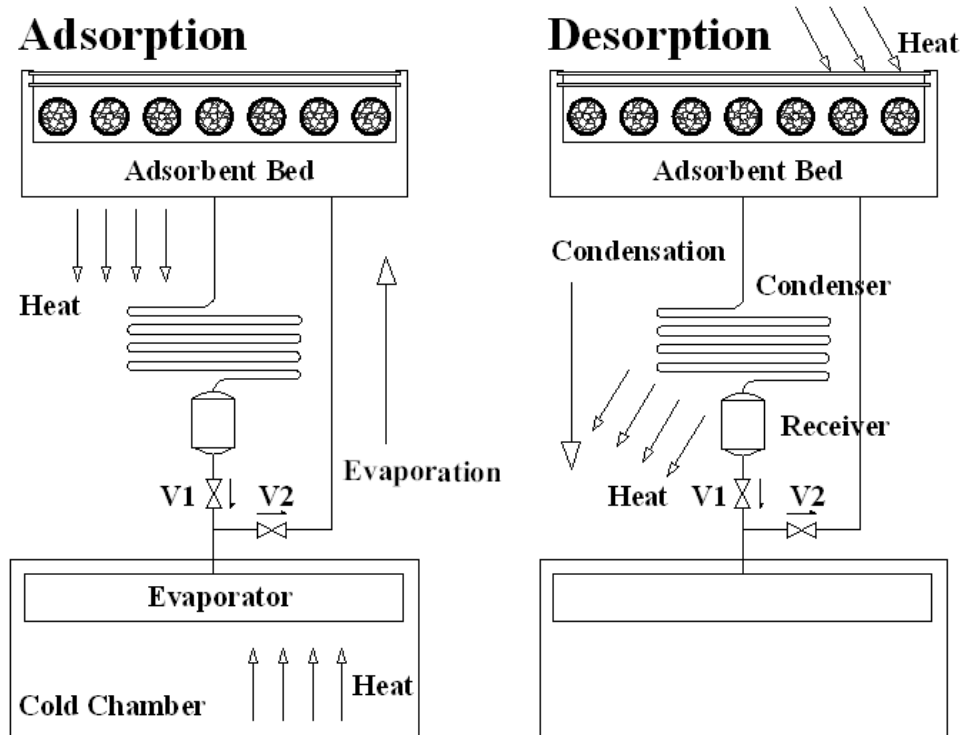
Figure 2
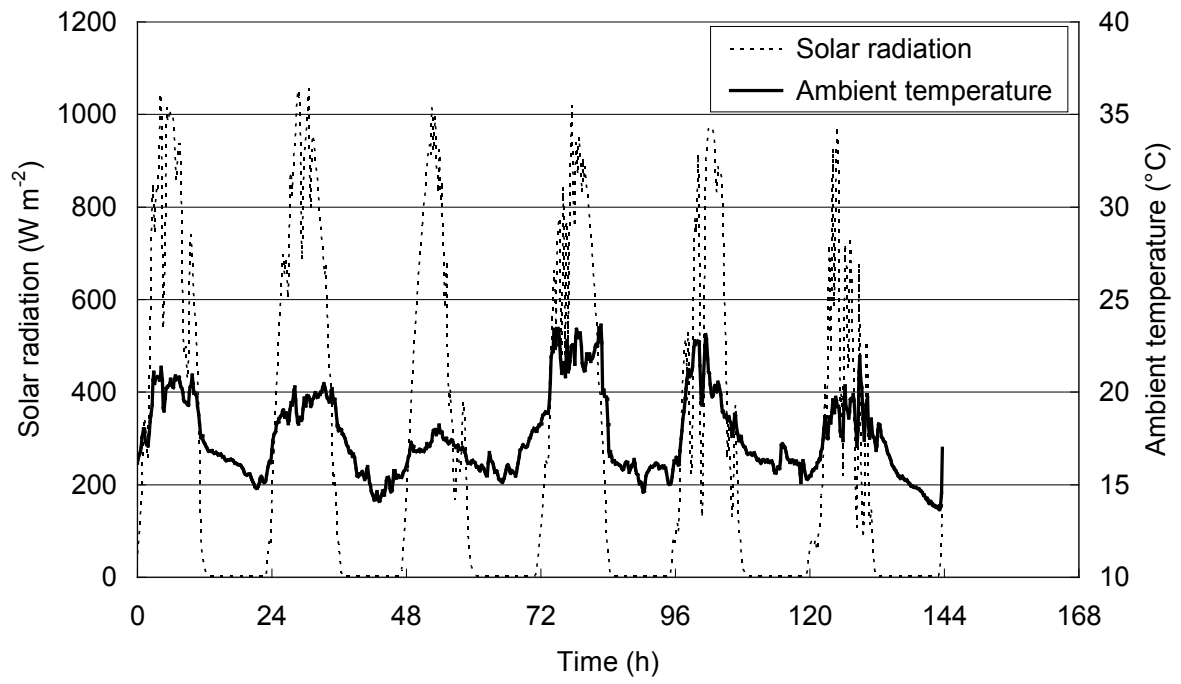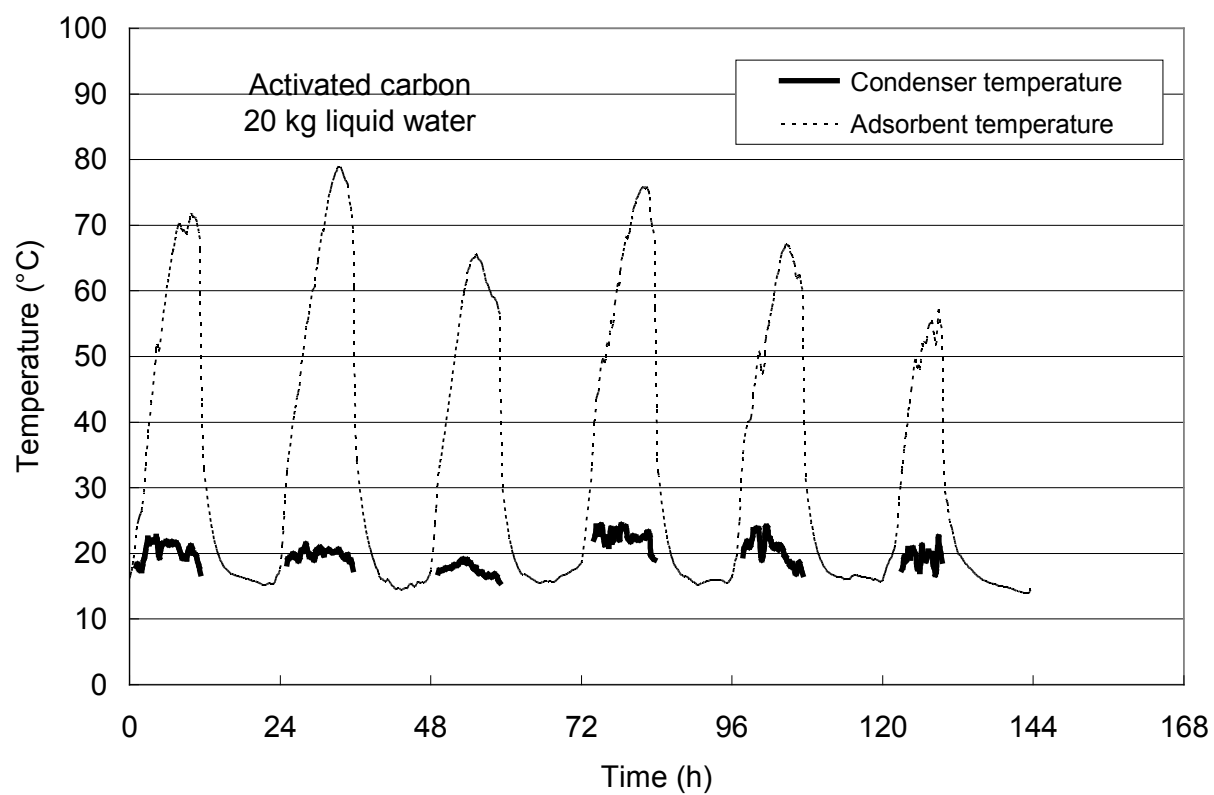
Figure 3

Figure 4
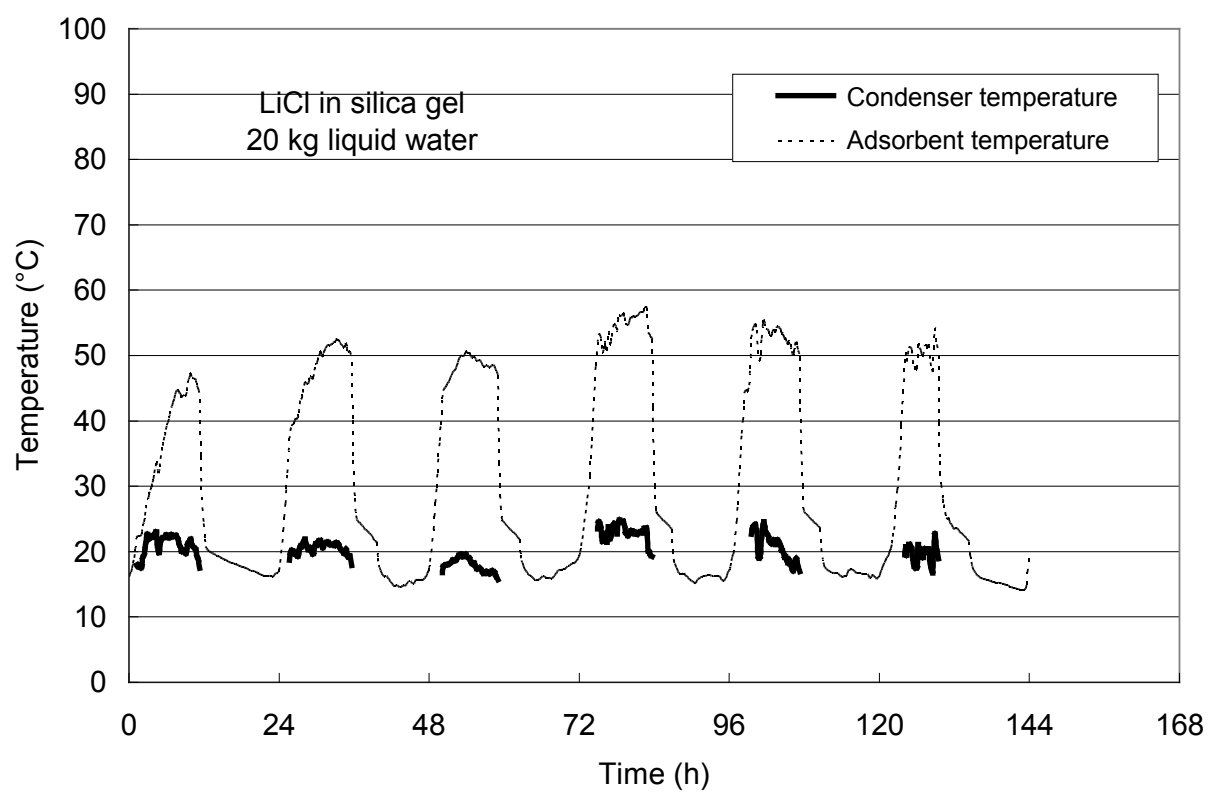
Figure 5
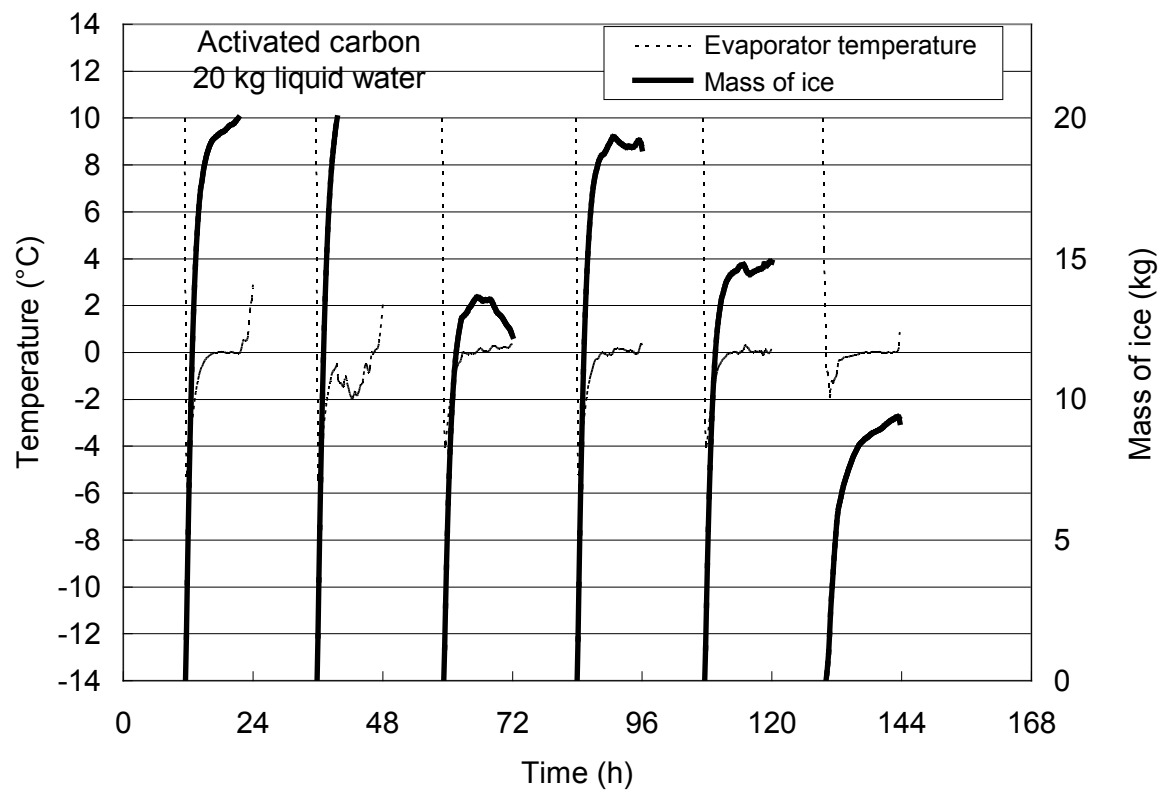
Figure 6
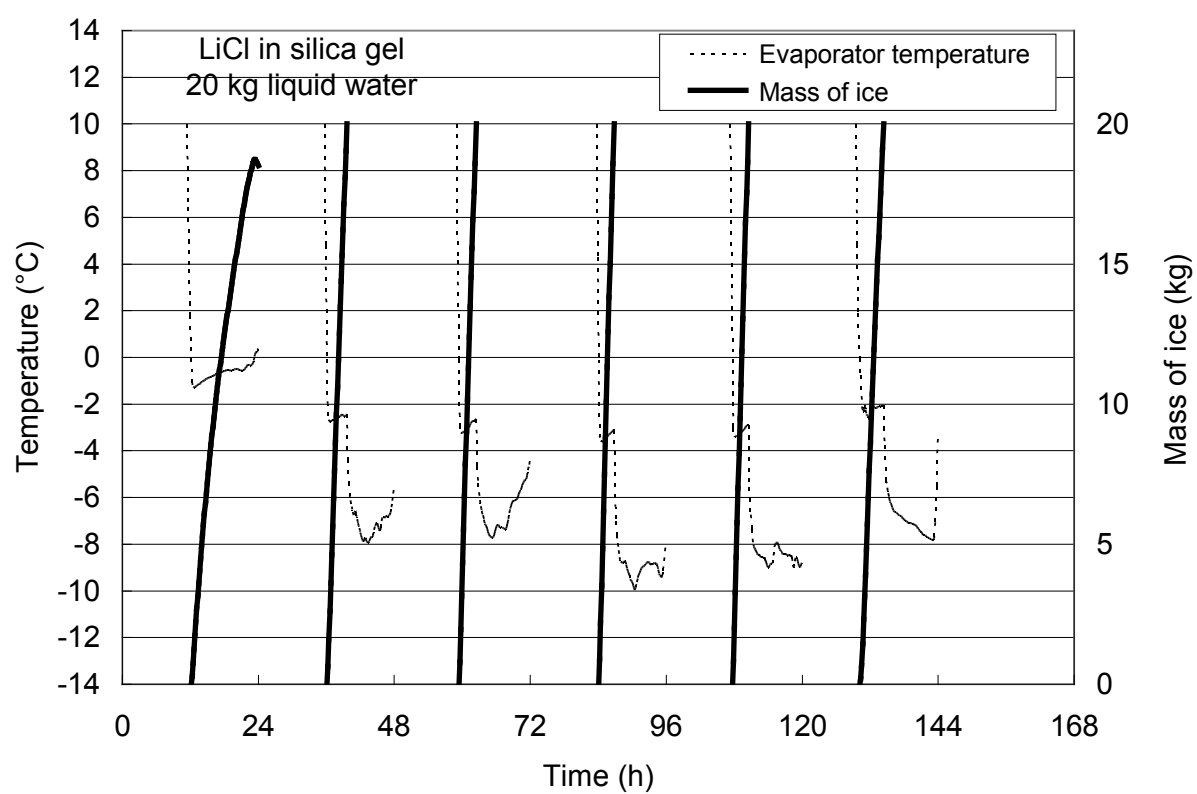
Figure 7

Figure 8

Figure 9